MAREZIO, M. (1966). *Acta Cryst.* **20**, 723.
MARGENAU, H. & MURPHY, G. M. (1956). *The Mathematics of Physics and Chemistry*. Princeton: Van Nostrand.
MERTENS, H.-E. v. & ZEMANN, J. (1966). *Acta Cryst.* **21**, 467.
NORRESTAM, R. (1968). *Ark. Kemi*, **29**, 343.
O'CONNOR, B. H. & VALENTINE, T. M. (1969). *Acta Cryst.* B**25**, 2140.
PATON, M. G. & MASLEN, E. N. (1965). *Acta Cryst.* **19**, 307.
PAULING, L. (1927). *J. Amer. Chem. Soc.* **49**, 765.
REITZ, J. R., SEITZ, R. N. & GENBERG, R. W. (1961). *J. Phys. Chem. Solids*, **19**, 73.
SAMSONOV, G. V. (1968). *Handbook of the Physicochemical Properties of the Elements*. New York: IFI/Plenum.
TEMPLETON, D. H. (1955). *J. Chem. Phys.* **23**, 1629.
TOSI, M. P. (1965). *Solid State Phys.* **16**, 1.
WILDE, D. J. (1964). *Optimum Seeking Methods*. Englewood Cliffs, N.J.: Prentice-Hall.
WYCKOFF, R. W. G. (1964). *Crystal Structures*, Vol. 2. New York: Interscience.

Acta Cryst. (1970). B**26**, 945

Structural Study of the Thorium Carbohydrides by X-rays and Proton Nuclear Magnetic Resonance: Evidence for Vacancy Induced Hydrogen Position Correlations

BY G. LOBIER

Centre d'Etudes Nucléaires, 92-Fontenay-aux-Roses, France

AND D. ROSSIER

Laboratoire de Physique des Solides, associé au C.N.R.S., Faculté des Sciences d'Orsay, 91-Orsay, France

(*Received* 19 *December* 1968)

The action of hydrogen on the hypo-stoichiometric monocarbides of thorium has been studied for various estimated carbon-vacancy contents in the homogeneity range of the carbide phase. The carbides can capture a considerable number of hydrogen atoms, and under saturation conditions, the ratio number of H_2 atoms/number of vacancies can be as high as 8. The structure of the carbohydrides remains f.c.c. during hydrogenation. The X-ray study of the variation of the cell parameter with hydrogen content showed it to behave very differently according to the initial carbon vacancy concentration. N.m.r. measurements likewise indicated, starting from certain hydrogen contents, a very rapid variation and exceptionally high values of the second moment calculated by integration of proton resonance spectra. These experimental results can be explained by the existence of strong correlations between the hydrogen atom positions in the carbohydride structure. These correlations would appear for sufficiently high hydrogen concentrations and are induced by the vacancies. They can be represented by configurations of pairs or triples of hydrogen atoms localized in the vicinity of the vacancy; the most probable configuration is that of pairs formed by one of the hydrogen atoms situated in the octahedral space left vacant by the missing carbon atom, the other being situated at one of the tetrahedral sites surrounding this vacancy.

The action of hydrogen on a certain number of the monocarbides of the transition metals Ti, Zr and Hf (Rexer & Peterson, 1964; Goretzki, Bittner & Nowotny, 1964; Goretzki, Ganglberger, Nowotny & Bittner, 1965; Yvon, Nowotny & Kieffer, 1967), and also on carbides of the lanthanide and actinide series, Y, Ho, Er, Th, U and Pu (Pascard, Lorenzelli & Dean, 1964) has already been observed. The hydrogenation of thorium carbides appears to be a complex process. Peterson & Rexer (1962) report the existence of two thorium carbohydrides $ThC.ThH_2$ (closed-packed hexagonal structure) and $ThC.2ThH_2$ (monoclinic) obtained by the action of hydrogen at 800°C on a low carbon-content ThC–Th mixture. However, Pascard *et al.* (1964) note that there is a reversible reaction of the single-phase thorium-rich monocarbide at medium temperatures (400°C), which gives rise to a face-centred cubic carbohydride structure by simple extension of the monocarbide unit cell. These structurally simple compounds form the subject of the present study. In particular, they offer favourable conditions for a study of the hydrogen atom positions in the lattice by nuclear magnetic resonance.

1. ACTION OF HYDROGEN ON THE THORIUM-RICH MONOCARBIDE

Experimental method

After having confirmed the absence of any reaction of hydrogen with the stoichiometric monocarbide ThC, we prepared a series of single-phased under-stoichiometric monocarbides. These compounds, which are obtained by direct reaction between the metal and a measured quantity of carbon, are prepared from a mixture of thorium hydride and graphite powder cold

compacted and sintered *in vacuo* (10^{-6} torr) at 1600 °C. The carbides were analysed as to carbon content by burning in a stream of oxygen and as to oxygen and nitrogen content by inert gas fusion. As these latter impurities replace the carbon atoms in octahedral positions, the vacancy proportion for each sample can thus be deduced. The lattice constants determined by the Debye–Scherrer X-ray method agree well with the literature (Aronson & Sadofsky, 1965; Satow, 1967). These results are given in Table 1.

Preparation of the carbohydrides

The carbohydrides were obtained by direct action of hydrogen at 450 °C on powdered samples, which were prepared by grinding the carbide pellets (first in a percussion mortar, then in an agate mortar) followed by sifting in a 30μ mesh sieve. These samples were placed in a vessel of known volume and degassed for three hours at 500 °C *in vacuo* (10^{-3} torr). A given quantity of high purity hydrogen (2 p.p.m. O_2, 2 p.p.m. N_2, 2 p.p.m. H_2O by volume) was introduced and this reacted with the sample, whose temperature was then gradually lowered from 450 °C to room temperature. The difference between the volume of hydrogen introduced and the volume of gas remaining in the vessel, reduced to standard temperature and pressure, enabled the quantity of hydrogen effectively absorbed by the carbide to be determined. The reaction tubes were sealed immediately and placed in an annealing furnace at temperatures ranging from 450 °C to room temperature. For n.m.r. measurements the annealed carbohydride was placed in a Pyrex tube under a purified argon atmosphere. The tube was then sealed under vacuum, after the absence of desorption at room temperature had been checked. After this treatment, the hydrogen content of the samples was verified by desorption *in vacuo* at 500 °C and the desorbed gas was stored in a Toepler pump.

Experimental results

An X-ray study was carried out concurrently with the n.m.r. measurements. The X-ray patterns were obtained on a Phillips camera from powders placed in Lindemann glass capillary tubes, filled and sealed in a glove box in a purified argon atmosphere. The lattice parameters were obtained from extrapolation to $\theta = 90°$ by the Nelson–Riley method. These experiments enable the crystallographic evolution of the carbohydride with increasing hydrogen content to be followed.

For any vacancy content of the initial carbide, the carbohydrides remain face-centred cubic. The variation in the lattice parameter a is given in Fig. 1. The hydrogen content is expressed by the ratio H/Th which, for the thorium monocarbide of NaCl-type structure, is equivalent to the ratio of the number of hydrogen atoms to the number of non-metallic octahedral positions.

When the hydrogen content is small, the hydrogenation of the carbide results in a simple modification of the parameter a, the high-angle X-ray lines remaining fine up to H/Th contents of 15 to 20 at.%. With higher hydrogen contents for which the variation of the parameter becomes important, it is not possible to obtain homogeneous samples at pressures of one to a few atmospheres, no matter how fine the powder is ground and how long the annealing continues. The high-angle lines of the X-ray patterns become blurred and the determination of the parameters less precise. This results in a variation of $\pm$5–10% in the hydrogen content of the sample. In addition, in order to obtain a satisfactory reproducibility in the parameter–concentration relation, it is essential to anneal the samples properly, so as to reduce the hydrogen concentration gradient from the boundaries to the centres of the grains. Nevertheless, when the saturation condition is approached, and the hydrogen pressures during annealing are about 10–15 atmospheres, good carbodride homogeneity can be achieved. This makes it possible to assess with satisfactory accuracy the unit-cell dimension of the saturated compound, which remains face-centred cubic. The analysis of the $a = f$(H/Th) curves (Fig. 1) suggests the following:

(1) The behaviour of the high vacancy monocarbides (in this case 16% vacancies) is characteristic:

Firstly, there is a slight contraction of the unit cell at low hydrogen contents which is not observed in the low vacancy compounds (4 and 7% vacancies).

Secondly, there is a significant variation in the parameter $a = 5{\cdot}318$ Å for high hydrogen contents (H/Th > 40%), which corresponds to a carbohydride unit-cell slightly larger in size than that of the stoichiometric monocarbide $ThC_{1{\cdot}00}$: $a = 5{\cdot}3430 \pm 5 \times 10^{-4}$ Å ($a = 5{\cdot}344$ Å according to Aronson & Sadofsky, 1965).

(2) On the other hand, with low vacancy mono-

Table 1. *Lattice parameters of various compositions of the monocarbide*

Theoretical composition	C (wt.%)	O_2 (wt.p.p.m.)	N_2 (wt.p.p.m.)	Measured composition	Vacancy concentration (%)	Parameter (Å)
$(ThC_{0{\cdot}8})^1$	3·88 ± 0·02	2900 ± 300	900 ± 100	$ThC_{0{\cdot}784}O_{0{\cdot}043}N_{0{\cdot}015}$	15·8 ± 1·0	5·3188 ± 5 10^{-4}
$(ThC_{0{\cdot}8})^2$	3·97 ± 0·02	2800 ± 300	900 ± 100	$ThC_{0{\cdot}800}O_{0{\cdot}042}N_{0{\cdot}015}$	14·3 ± 1·0	5·3260 ± 3 10^{-4}
$(ThC_{0{\cdot}9})$	4·48 ± 0·02	1200 ± 150	340 ± 40	$ThC_{0{\cdot}908}O_{0{\cdot}018}N_{0{\cdot}006}$	6·8 ± 0·7	5·3390 ± 3 10^{-4}
$(ThC_{0{\cdot}95})$	4·64 ± 0·02	1900 ± 200	200 ± 20	$ThC_{0{\cdot}934}O_{0{\cdot}028}N_{0{\cdot}003}$	3·5 ± 0·72	5·3422 ± 3 10^{-4}

carbides, even those with very high hydrogen contents such as H/Th = 0·57 for ($ThC_{0·9}$) and H/Th = 0·29 for ($Th_{0·95}$) which correspond respectively to the ratios hydrogen/vacancy = 0·57/0·068 ≃ 8 and 0·29/0·035 ≃ 8, the hydrogen atoms occupy the carbide unit-cell without dilating it unduly: $\Delta a \simeq 6 \times 10^{-3}$ Å for ($ThC_{0·9}$) at the saturation condition whereas it is insignificant for ($ThC_{0·95}$).

The hydrogenation process calls for a number of comments:

(1) The phenomenon is reversible and, irrespective of the lack of homogeneity in the carbohydride, the desorption process restores a perfectly crystallized compound which is identical to the original carbide. However, the parameters of the compounds obtained by desorption at 500 °C and at $\sim 10^{-3}$, 10^{-4} torr differ slightly from the parameters of the initial carbides. The ($ThC_{0·8}$)H_y carbides systematically give rise to desorbed compounds having slightly smaller parameters than that of the original carbide: $a = 5·316 \pm 10^{-3}$ Å for $(ThC_{0·8})^1$ or $\Delta a = -0·0028 \pm 10^{-3}$ Å.

The carbohydrides ($ThC_{0·9}$)H_y when desorbed have a parameter slightly exceeding that of the initial carbide, *i.e.* $a = 5·3405 \pm 5 \times 10^{-4}$ Å, then $\Delta a = +0·0015 \pm 5 \times 10^{-4}$ Å.

This does not affect the reversibility of the process and may be explained from the curves of Fig. 1. With small hydrogen contents the carbohydride remains stable under the previously mentioned desorption conditions and the hydrogen is not completely released.

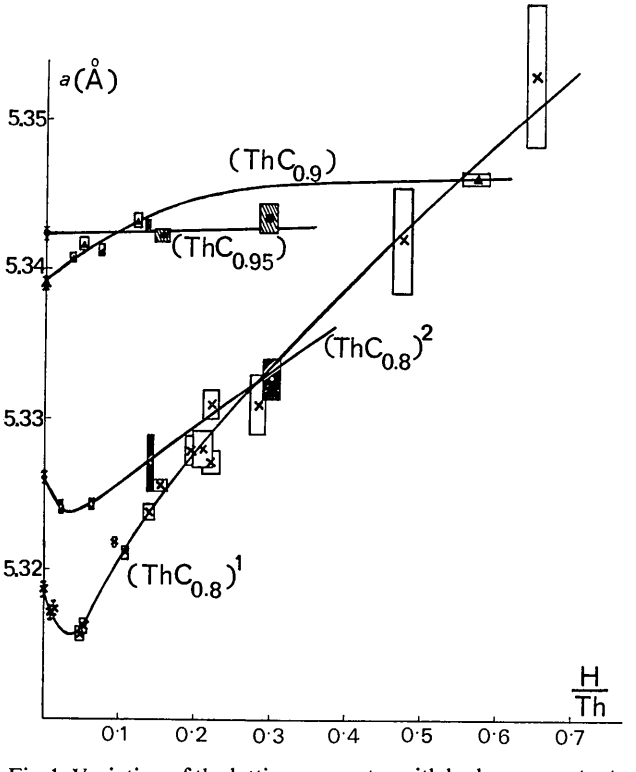

Fig. 1. Variation of the lattice parameter with hydrogen content.

This agrees well with the observed fact that hydrogen contents determined by desorption under the preceding conditions are slightly, but systematically, less than the contents determined immediately on absorption.

It is also observed that the hydrogenation mechanism is linked to the existence of carbon vacancies, since the hydrogen only reacts with the monocarbide if it is under-stoichiometric. This is not just a qualitative relation since the total quantity of hydrogen absorbed drops as the proportion of vacancies decreases. However, there is no strict quantitative relation between this proportion and the concentration of hydrogen in the saturated carbohydride, and the hydrogenation limit in the range of high hydrogen contents is very difficult to assess owing to extremely slow absorption at atmospheric pressure. However, the carbohydride approaching saturation point is obtained more easily with a low vacancy compound (7 and 4%) and corresponds to ratios of hydrogen/vacancy approximating to 8, whereas with a vacancy proportion of 16% it is difficult, under atmospheric pressure, to exceed the ratio of hydrogen/vacancy = 6, beyond which the reaction kinetics are extremely slow.

These comments suggest intuitive assumptions as to the position of the hydrogen atoms in the carbohydride unit cell. As there is a link between the hydrogenation process and the presence of vacancies it is quite logical to assume that the hydrogen atom might prefer to occupy a position near the vacancy. Two types of position are then available to it: (*a*) the octahedral position made vacant by the absence of a carbon atom and (*b*) the tetrahedral positions surrounding this vacancy, access to which is facilitated by the central octahedral hole. A precise description of these positions will be given later on. However, the existence of dense clusters of hydrogen atoms forced into a vacancy is quite meaningless from a physical point of view. Simply by considering the high values of H/Th ≃ 8 at the saturation condition, we can assume that the hydrogen atoms cannot be accommodated by octahedral positions only. Furthermore, the evolution of the parameters with respect to hydrogen content (Fig. 1) shows that the influence of the hydrogen on the lattice varies widely according to the number of vacancies in the original carbide. The n.m.r. technique seemed to us to be a way of providing useful data on the H–H distances and thence on the spatial distribution of hydrogen atoms.

2. N.M.R. MEASUREMENTS

N.m.r. has been used in the case of hydrides of transition metals, to determine both the atomic structure (distribution of the hydrogen atoms over the interstitial sites of the matrix) (Stalinski, Coogan & Gutowsky, 1961; Zamir & Cotts, 1964; Stalinski & Zogal, 1965; Bittner, 1964) and electronic structure (Knight shift measurement) (Oriani, McClement & Youngblood, 1957; Betsuyaku, Takagi & Betsuyaku, 1964) and also for studies of self-diffusion of hydrogen in the

lattice (Zamir & Cotts, 1964; Stalinski & Zogal, 1965; Zogal & Stalinski, 1966; Torrey, 1958). A number of experiments involved highly hydrogenized systems of the MH_x type, where x is the hydrogen content and M a transitional metal at the beginning of the series such as Ti, V, Nb or Ta. In such cases, the presence of hydrogen in the metallic lattice modifies the atomic structure itself, thereby giving rise to one or more new phases.

The information gathered from these experiments mainly concerns the self-diffusion of the hydrogen atoms, which generally occurs at high temperature. The second moment* values of the low temperature n.m.r. spectrum of the protons give frequently ambiguous information on the distribution of the hydrogen atoms over the various positions since, as far as most of these experiments are concerned, the metallic nuclei have a non-zero nuclear spin and the second moment includes a dipole interaction term between the spins of the protons and those of the other nuclei. This term can be dominant or of the same order as the proton–proton dipole interaction term, which is the only one able to provide information on the distribution of the protons over their positions. This is shown explicitly in the second moment expression calculated by the van Vleck method (Abragam, 1961):

$$M_2=\langle \Delta H^2\rangle=\tfrac{3}{5}I(I+1)\gamma_I^2\hbar^2\sum_j \mathbf{r}_j^{-6} + \tfrac{4}{15}S(S+1)\gamma_S^2\hbar^2\sum_k \mathbf{R}_k^{-6}, \quad (1)$$

$I=\frac{1}{2}$ = proton spin, S = spin of the other nuclei, γ_I and γ_S = gyromagnetic ratios of the protons and other nuclei respectively, $\mathbf{r}_j$ and $\mathbf{R}_k$ are the vector radii joining a given proton to the positions occupied by another proton ($\mathbf{r}_j$) or by another nucleus ($\mathbf{R}_k$). The sums $\sum_j$ and $\sum_k$ refer only to the positions occupied. In the system that we have studied, *i.e.* $ThC_{1-x}H_y$, the spin S of the nucleus ^{232}Th is zero, which greatly simplifies matters. It should be noted that there are of course the spins of the ^{13}C nuclei, but they have an isotopic abundance of only 1·1%. The calculation of the second moment due to these spins gives: $M_2 \simeq 0{\cdot}005$ (Gauss)^2, which is two or three orders of magnitude less than the second moments we measured. It may thus be considered that the spins of the ^{13}C nuclei are not important.

Atomic structure and available positions

Unlike a pure metal, fully stoichiometric thorium carbide cannot be hydrogenized. To be hydrogenized the carbon atom lattice must have vacancies. When this condition is fulfilled, up to about eight times more hydrogen atoms than carbon vacancies may be introduced. One can imagine the vacancies as being like doors which, when they are open, let in a great number of hydrogen atoms. However, even when highly hydrogenized, the carbon lattice remains of the NaCl type, and only the lattice parameter changes (see above). The thorium-rich carbide structure being of the NaCl type, two kinds of position are available for the hydrogen atoms (Fig. 2).

First there are the tetrahedral positions $(\frac{1}{4},\frac{1}{4},\frac{1}{4})$, of which there are 8 per unit cell in a hard sphere model where the Goldschmidt radius of the thorium atom is $r_{Th}=1{\cdot}8$ Å and that of hydrogen atom 0·46 Å. The tetrahedral position is compact, in so far that there is contact between the hydrogen sphere and the four adjacent thorium spheres. This can be seen by noting that the distance between a tetrahedral site and a metallic first-neighbour site $\frac{\sqrt{3}}{4}a=2{\cdot}3$ Å when the parameter of the unit cell is $a=5{\cdot}3$ Å. Whence $\frac{\sqrt{3}}{4}a-r_{Th}=0{\cdot}5$ Å, which is close to the atomic radius of hydrogen. It is obvious that such a model has a physical meaning only if the hydrogen atoms are not ionized. However, a hydrogen–thorium distance of about 2·3–2·4 Å has already been found in various other thorium–hydrogen compounds (Zachariasen, 1953). Furthermore, in the case of the dihydride, neutron diffraction studies show the hydrogen position to be tetrahedral (Rundle, Shull & Wollan, 1952). The lattice of these tetrahedral positions is simple cubic, with parameter $\frac{a}{2}=2{\cdot}67$ Å.

Secondly, the absence of a carbon atom releases space of octahedral symmetry, which is available for the hydrogen atoms. In a hard sphere model, the most compact positions which may be occupied by hydrogen

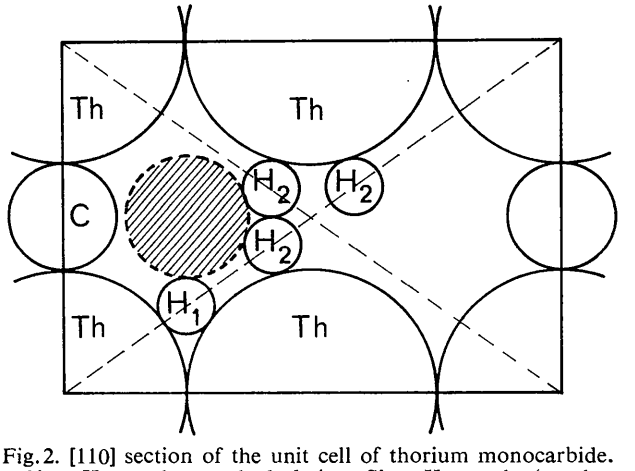

Fig. 2. [110] section of the unit cell of thorium monocarbide. Sites H_1 are the tetrahedral sites. Sites H_2 are the 'octahedral' sites available within the vacancy. The hydrogen atoms cannot enter the shaded circle.

* The second moment of a spectral line, defined by the function $f(H)$ of the applied magnetic field H and centred in the field H_0, is defined by

$$M_2=\langle \Delta H^2\rangle=\int f(H)\,(H-H_0)^2 \mathrm{d}H \Big/ \int f(H)\mathrm{d}H\,.$$

atoms are the corners of a cube centred on the octahedral position, and of side 1 Å (see Fig. 2). The symmetry of the positions thus defined is less than that of tetrahedral sites. For convenience shall call this type of position 'octahedral', whereas we call the geometrical centre of the vacancy a 'fictitious octahedral site'.

Effect of temperature

The n.m.r. measurements were carried out at the temperature of liquid helium, between 4·2 and 1·4°K. It may then be assumed that the hydrogen atoms form a 'rigid' lattice, in so far that any possible movements of the protons occur over a much longer time scale than the Larmor period τ_L, which in the present case is $\sim 3 \times 10^{-8}$ sec. To justify this one can use a simple model in which the position to position jump frequency is given by an Arrhenius type formula:

$$\nu = \nu_0 \exp\left[-E_a/kT\right],$$

where ν_0 is a characteristic frequency and E_a the activation energy for diffusion between neighbouring positions. When ν exceeds $1/\tau_L$, the rapid relative movements of the nuclei reduce the time average of the spin–spin dipole interactions. The line is narrowed by the movement. To give an idea of the order of magnitude, the values of ν_0 and E_a measured on a number of hydrides (Zamir & Cotts, 1964; Zogal & Stalinski, 1966) are:

$\nu_0 \simeq 10^{11}$–10^{-12} sec^{-1}, and $E_a \simeq$ several kcal.mole^{-1}.

For $\nu\tau_L \simeq 1$ the corresponding temperatures are of the order of a few hundred degrees Kelvin. Below these temperatures the width of the measured line δH differs very little from that calculated for a rigid lattice δH_0. This is illustrated by the $\delta H/\delta H_0$ ratio for $kT \ll E_a$, as calculated using the Kubo & Tomita (1954) formula:

$$\nu = 2\,(\log 2)^{1/2}\,(\gamma\,\delta H)/\mathrm{tg}\left[\frac{\pi}{2}\,(\delta H/\delta H_0)^2\right],$$

in which, when $\nu \to 0$ at low temperature, $\delta H/\delta H_0 \to 1$.

With liquid helium, we are certainly very much below the characteristic narrowing temperatures. In fact, apart from intensity, no variation of the spectrum was observed experimentally between 4·2 and 1·4°K in the $ThC_{1-x}H_y$ system.

In summary, the system we have studied may be characterized by an arrangement of spins $I=\frac{1}{2}$, all identical, spread 'rigidly' over a lattice of positions to be determined. As a first variable parameter, there is the available dilution of protons on their positions, but we shall see that the carbon atom vacancy content also plays an important role.

Experimental method

The resonant absorption of the steady state proton spins was observed by the Q-meter method. At low temperature the longitudinal relaxation of the protons is very slow and in order to prevent the signal becoming saturated it was necessary to work at low resonant frequency levels of 10 to 50 mV as measured on the coil in which the sample was placed. Measurements were made at a Larmor frequency of ~35 Mc sec^{-1}. The frequency drift was ≤ 5 c sec^{-1} per minute. The magnet was a 12 inch Varian. The homogeneity of the magnet and its drift were measured on a mineral oil sample of the same dimensions as the carbide samples (5 mm diameter × 15 mm long). At 8 kG, the inhomogeneity was less than 100 m Gauss and the drift less than 5 m Gauss/mn.

In fact, the principal contribution to magnetic inhomogeneity is the sample itself. This is due to the fact that small ferromagnetic particles are almost inevitably introduced during the preparation. Their presence in the samples is revealed in three different ways.

(1) Magnetic susceptibility measurements show that there was a ferromagnetic type contribution. No paramagnetic contribution at low temperature was found.

(2) The chemical determinations carried out on the samples used for the susceptibility measurements yielded concentrations of 150 to 200 p.p.m. of iron and 150 p.p.m. nickel. The ferromagnetic contribution to the susceptibility indicates that the greater part of the impurities which are likely to be magnetic must be in a free state.

(3) This is confirmed by n.m.r. measurements. The nuclear resonance at room temperature from protons contained in a few drops of mineral oil intimately mixed in two different thorium carbide samples has been observed. The significant broadening of the proton lines of the mixed oil is obvious, as compared with that of the pure oil. This broadening must therefore be attributed to a macroscopic inhomogeneity, such as may be caused by ferromagnetic particles. The second moment measured on the proton lines of the oil mixed with the powder is $0{\cdot}25 \pm 0{\cdot}05$ (Gauss)^2. The peak-to-peak width of the derivative of the line is about 0·7 Gauss, whereas in the case of the pure oil it is considerably less than 0·1 Gauss. Assuming that the ferromagnetic particles are homogeneously distributed in the sample, it is found that 200 p.p.m. of impurities, each of $1\mu_B$, create an average inhomogeneity of $\frac{1}{2}$ Gauss, which agrees with the width of the inhomogeneous line measured.

Experimental results

The n.m.r. spectrum of the protons was measured on three series of samples taken from among the carbides described in §1. The parameters of the carbohydrides used for n.m.r. experimentation fall on the previously plotted **a** parameter–concentration curves. They are designated by:

series a: $(ThC_{0{\cdot}8})^1$, $(ThC_{0{\cdot}8})^2$

series b: $(ThC_{0\cdot9})$
series c: $(ThC_{0\cdot95})$

corresponding to ratios $x = \frac{\text{number of vacancies}}{\text{number of Th atoms}}$: 0·16, 0·07 and 0·04 respectively. The ratios $y = \frac{\text{number of H atoms}}{\text{number of Th atoms}}$ are reported in Table 2 for each sample.

The peak-to-peak width of the derivative was measured on each resonance line. By integrating the spectrum, the second-moment value was also determined (see Table 2 and Fig. 4). The three types of line involved, depending on the hydrogen concentration, are illustrated in Fig. 3. The narrow line (*a*) corresponds to the samples in which the hydrogen is very dilute, the broad line (*c*) to those greatly hydrogenized. Lastly, line (*b*), of complex form, represents intermediate concentrations. It seems to result from the superimposition of two lines, the narrower one having a peak-to-peak width similar to the lines of the diluted samples, whereas the wide broad line resembles that of greatly hydrogenized samples. This kind of line was found in samples 2*a* and 3*a* of series *a*. This type of structure does not appear in series *b* and *c* at the concentrations available.

Examination of Table 2 and Fig. 4 leads to the following:

(1) At low concentrations ($y \simeq$ a few per cent), the line width and the second moment appear to be concentration independent (see for instance series *b*).

(2) With the intermediate concentration (10 to 20%) there is a rather sharp variation of the second moment. For instance, in the case of series *a*, this is due to the appearence of wings spreading out each side of the line. The concentrations where this rapid variation occurs depend on the proportion of carbon vacancies.

Thus, with a high proportion of vacancies (series *a*), there is a very clear increase in the second moment beginning at 7% hydrogen atoms, whereas in the two other series, where the vacancy content is respectively twice and four times less, for 12% of hydrogen atoms, the second moment is still small and no wings have appeared.

Interpretation

At low hydrogen concentrations when the dipole second moment of the protons is less than 0·25

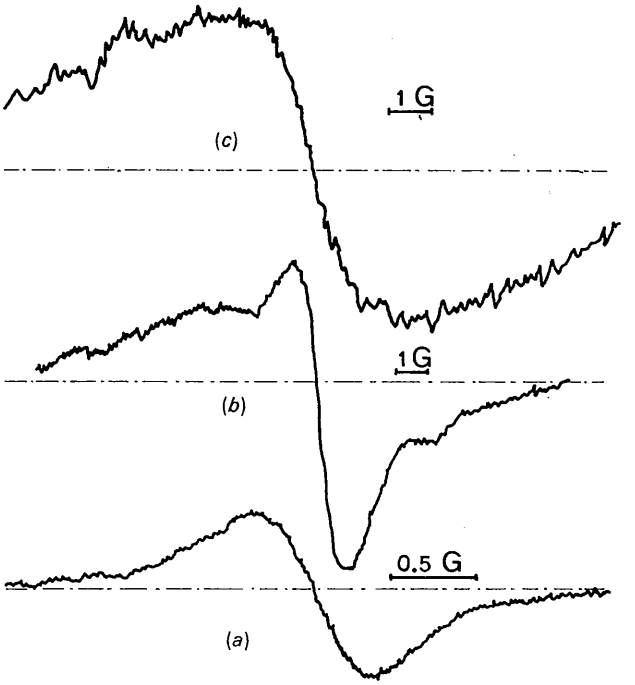

Fig. 3. Derivative of the nuclear absorption at 35 Mc.sec^{-1} frequency: (*a*) sample 5*a* $(ThC_{0\cdot8}H_{0\cdot014})$; (*b*) sample 3*a* $(ThC_{0\cdot8}H_{0\cdot094})$; (*c*) sample 1*c* $(ThC_{0\cdot95}H_{0\cdot29})$.

Table 2. *Results of the n.m.r. experiments*

Sample	Ratio vacancy/ thorium atom	Ratio hydrogen atom/ thorium atom	Ratio hydrogen atom/ vacancy	Peak to peak width (Gauss)	Second moment (Gauss)^2
1*a*	0·15 ± 0·01	0·30 ± 0·01	2·00	6·5 ± 0·5	16·7 ± 0·4
2*a*	0·15 ± 0·01	0·140 ± 0·003	0·93	*	4·4 ± 0·2
3*a*	0·16 ± 0·01	0·094 ± 0·0015	0·59	*	3·6 ± 0·3
4*a*	0·15 ± 0·01	0·063 ± 0·0012	0·42	1·1 ± 0·1	0·55 ± 0·15
5*a*	0·16 ± 0·01	0·0143 ± 0·0002	0·087	1·2 ± 0·1	0·23 ± 0·01
1*b*	0·07 ± 0·007	0·57 ± 0·01	8	7 ± 0·5	18·5 ± 1
2*b*	0·07 ± 0·007	0·120 ± 0·005	1·71	0·7 ± 0·1	0·34 ± 0·01
3*b*	0·07 ± 0·007	0·032 ± 0·001	0·46	0·65 ± 0·1	0·20 ± 0·05
4*b*	0·07 ± 0·007	0·009 ± 0·0009	0·13	0·6 ± 0·15	0·26 ± 0·02
5*b*	0·07 ± 0·007	0·049 ± 0·001	0·70	0·7 ± 0·1	†
6*b*	0·07 ± 0·007	0·074 ± 0·002	1·06	0·65 ± 0·05	0·25 ± 0·05
1*c*	0·04 ± 0·007	0·295 ± 0·015	7·4	4·5 ± 0·5	10 ± 1
1*c*	0·04 ± 0·007	0·127 ± 0·003	3·2	0·7 ± 0·15	0·16 ± 0·01
1*c*	0·04 ± 0·007	0·033 ± 0·002	0·08	0·7 ± 0·2	

* Complex structure.
† Not measurable owing to a weak signal to noise ratio.

(Gauss)², all information is lost owing to the inhomogeneous broadening due to ferromagnetic particles. This explains why the width of the line does not vary and why the second moment stays at about 0·2–0·3 (Gauss)² in these conditions. The quantitative interpretation is therefore limited to hydrogen concentrations leading to a second moment of more than 0·3 (Gauss)².

This being so, the measured second moments can be compared with those calculated from models of hydrogen atom distribution on the two types of position described above (see the section *Atomic structure and available positions*).

A first type of model assumes that there is a random distribution of the atoms over the positions. The second-moment value is then expressed by the formula (Abragam, 1961, p. 133)

$$M_2 = f\tfrac{3}{5}I(I+1)\gamma_I^2\hbar^2 \sum_j \mathbf{r}_j^{-6}$$

where f is the dilution on positions $\mathbf{r}_j$.

The second moment thus evaluated with respect to the ratio $y = \mathrm{H/Th}$ is found to be (*a*) $1{\cdot}8y$ (Gauss)² for the fictitious octahedral positions alone, (*b*) $4{\cdot}2y$ (Gauss)² for the tetrahedral positions alone and (*c*) $9{\cdot}8y$ (Gauss)² for the hydrogen atoms randomly distributed over both types of position together. By assuming inequivalent repartition of the hydrogen atoms on both types of site, intermediate values are found given by the formula (Bittner, 1964)

$$M_2 = 1{\cdot}8y[1 + 18{\cdot}87(\beta/y) - 32{\cdot}42(\beta/y)^2] \qquad (d)$$

where β is the probability of finding a hydrogen atom on a tetrahedral site, and y is the hydrogen concentration expressed as an atomic percentage. The expressions (*a*), (*c*) and (*d*) do not take account of the presence of carbon atoms on most of the octahedral sites. For instance, (*a*) cannot be used when y is larger than the vacancy concentration. The comparison with the second moment values observed (see Fig. 4) shows that:

(1) For the three series *a*, *b*, *c*, and with concentrations of over 20% these models yield moment values that are much too small. Nevertheless it may be noted that the observed values are of the same order of magnitude as the values calculated in the case of saturation of tetrahedral sites or both tetrahedral and octahedral sites. This means that in the carbohydrides investigated the hydrogen interatomic distances involved are comparable with those for the case where the above sites are imagined to be saturated. Therefore there are strong correlations between the positions of the hydrogen atoms in the carbohydride structure which tend to bring them closer together than they would be in a simple model of random distribution, which results in an increase in the second-moment value.

(2) If one now considers the intermediate concentrations $10\% \leq y \leq 20\%$, a very remarkable difference is noticed between the series *a* with a very high vacancy density (16%) and those with a low density *b*: 7% and *c*: 4%. The correlations between the hydrogen positions do not come into play in the case of the last two series, whereas they certainly do in the first, since the second-moment value is already very much higher than in the random model. Furthermore, in this high vacancy density series a complex form of the line [Fig. 3(*b*)] appears which seems to result from at least two different types of position, whereas nothing like this occurs with low vacancy-content samples having the same absolute number of hydrogen atoms. Thus the two following initial conclusions are reached: when the hydrogen concentration is raised, their positions are correlated and the greater the number of vacancies, the greater is the correlation. The simplest way of introducing correlations into a crude model is to assume that the hydrogen atoms tend to form pairs. In this model the second moment value is equal to that of the pair, plus the correction for the effect of the other neighbouring pairs. If this last correction is ignored, the second-moment value of the line of an isolated pair of protons separated by a distance r is $M_2 = \frac{4}{5}\left[\frac{3}{4}\gamma\frac{\hbar}{r^3}\right]^2$ (Pake, 1948). The values of M_2 thus calculated for the various types of pairs, according to

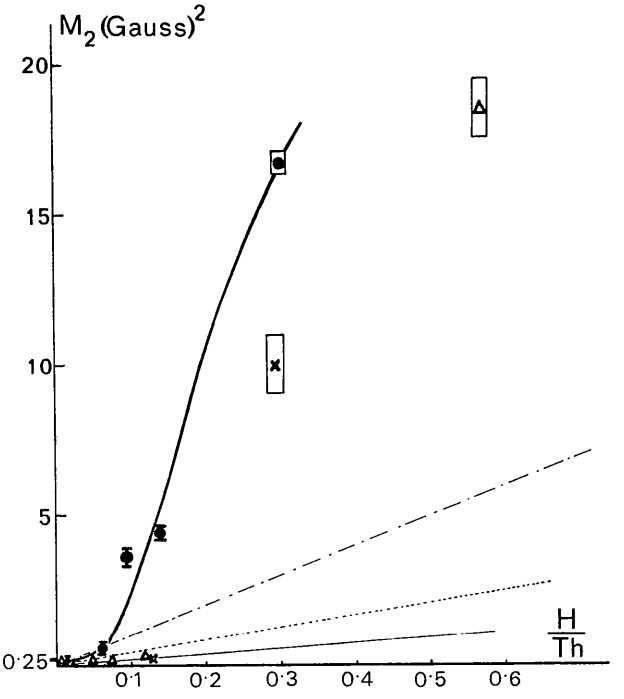

Fig. 4. Variation of the second moment, M_2, of the proton line *versus* hydrogen content. ●, series *a*; △, series *b*; ×, series *c*. For comparison the calculated second moment is drawn for a random distribution on ——·—, fictitious octahedral sites; ·····, tetrahedral sites; ------, both tetrahedral and fictitious octahedral sites. The value of the spurious magnetic inhomogeneity due to ferromagnetic particles is 0·25 (Gauss)².

the sites occupied by each proton forming a pair, are given in Table 3. The significant figures are the weighted averages over all the configurations of one type of pair. It will be seen that the only types of pairs which can be considered to explain the line widths observed at high hydrogen concentrations are the 'mixed pairs', that is to say the pairs in which one of the protons is on one of the positions made available by an octahedral vacancy and the other on a tetrahedral position in the vicinity of the vacancy [see Fig. 5(*d*)]. The pairs located solely on tetrahedral positions [Fig. 5(*a*)] or solely on fictitious octahedral positions [Fig. 5(*b*)] give values that are much too small whereas the pairs located within the same vacancy give values that are far too great [Fig. 5(*c*)]. This model could be refined by introducing hydrogen triplets (two protons in tetrahedral sites in the vicinity of a vacancy occupied by one proton) which in fact certainly exist at high hydrogen concentrations. The n.m.r. spectrum of a triplet has been calculated only in the case of an equilateral configuration (Andrew & Bersohn, 1950). In this case the second-moment value is double that of a pair for the same distances between protons. Finally the contribution to the second moment due to the influence of adjacent pairs or triplets should be allowed for. The second-moment value calculated from all these configurations of mixed pairs and triplets or even higher-order clusters is of the order of magnitude observed at high concentrations for series *a*, *b* and *c*. For the samples 2*a* and 3*a*, it is possible that the narrow line remaining in the spectrum [Fig. 3(*b*)] may correspond to as yet unpaired hydrogen atoms.

Conclusions

The experimental results can be semi-quantitatively explained with a model of position correlations between hydrogen atoms, or more precisely, of correlations induced by the vacancies. As a first approximation the correlations may be described in terms of pairs of hydrogen atoms, one of which is in the space of a vacancy and the other in one of the tetrahedral positions surrounding the vacancy.

The first property of this correlation is that it appears fairly sharply at a certain hydrogen concentration range. Below this transition interval the probability of the hydrogen atoms forming the pairs described above is small and, owing to the inhomogeneous magnetic broadening of the line, it is not possible to indicate exactly what position these pairs will occupy. The problem may be understood physically by saying that the correlations, which must be short range, only come into play when the hydrogen atoms are sufficiently numerous to come together and form a pair.

The second property of the correlation is that it is more easily induced as the number of carbon vacancies in the lattice increases. The physical interpretation of this phenomenon is not obvious, for when the number of vacancies is greatly increased their lattice becomes multiply connected. This is entirely so for the 80% carbon atom series where a simple statistical count shows that only about 6% of the vacancies have no immediate neighbours, whereas about 80% form connected clusters of more than 3 vacancies. Under these conditions any description based on an isolated vacancy loses its significance and the interpretation of the phenomenon is more complicated. It is possible that the great number of vacancies helps the forming of 'mixed' pairs for purely geometrical reasons, their multiply-connected lattice making it easier for the protons to diffuse to form 'mixed pairs'. But it is also possible that the presence of a great number of vacancies strongly disturbs the wave function of the hydrogen atoms, so that correlation between the hydrogen atoms is strengthened. Incidentally, the fact that the concentration of vacancies has an important effect on the lattice is particularly noticeable on the curve giving the variation of the lattice parameter (see §1).

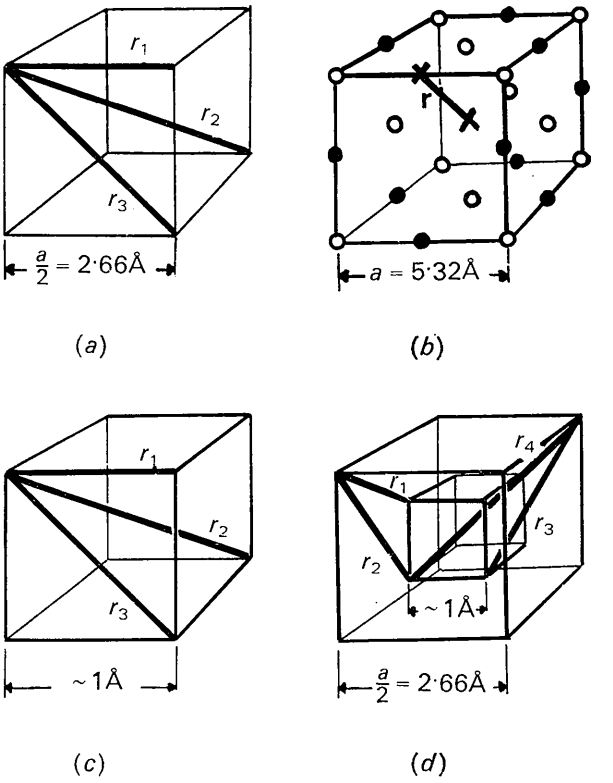

Fig. 5. Interatomic distances for different configurations of hydrogen pairs. (*a*) Pairs of hydrogen atoms on two neighbouring tetrahedral sites, $r_1 = 2{\cdot}66$, $r_2 = 3{\cdot}75$, $r_3 = 4{\cdot}6$ Å. (*b*) Pairs of hydrogen atoms on two neighbouring fictitious octahedral sites, $r = 3{\cdot}7$ Å. ○, thorium; ●, carbon; ×, hydrogen. (*c*) Pairs of hydrogen atoms within the same vacancy, $r_1 = 0{\cdot}96 \pm 0{\cdot}04$, $r_2 = 1{\cdot}35 \pm 0{\cdot}05$, $r_3 = 1{\cdot}65 \pm 0{\cdot}05$ Å. (*d*) Mixed pairs of hydrogen atoms: one atom occupying a corner of the small cube, *i.e.* one of the 'octahedral' sites, the other occupying a corner of the large cube, *i.e.* one of the first-neighbour tetrahedral sites. $r_1 = 1{\cdot}5$, $r_2 = 2{\cdot}17$ $r_3 = 2{\cdot}65$, $r_4 = 3{\cdot}10$ Å.

Table 3. *ΔH and M_2 for the various types of site and hydrogen atom pairs*

Type of site	Peak-to-peak width ΔH (Gauss)	Second moment M_2 (Gauss)^2
Fictitious octahedral sites dilution $= H/\mathrm{Th} = y$	$2{\cdot}68\sqrt{y}$	$1{\cdot}8y$
Tetrahedral sites dilution $= y/2$	$4{\cdot}1\sqrt{y}$	$4{\cdot}2y$
Fictitious octahedral + tetrahedral sites dilution $= y/3$	$6{\cdot}27\sqrt{y}$	$9{\cdot}8y$

Type of pair*	Interatomic distances	Peak-to-peak width ΔH (Gauss)	Second moment M_2 (Gauss)^2
Hydrogen atoms on two neighbouring tetrahedral sites [Fig. 5(*a*)]	r_1	2·27	1·03
	r_2	0·8	0·13
	r_3	0·42	0·035
		†$\Delta H_{\text{average}} = 1{\cdot}37$	†$M_{2\text{average}} = 0{\cdot}5$
Hydrogen atoms within the same vacancy [Fig. 5(*c*)]	r_1	48 ± 6	450 ± 100
	r_2	$17{\cdot}1 \pm 1{\cdot}1$	57 ± 17
	r_3	$9{\cdot}4 \pm 0{\cdot}8$	$20{\cdot}4 \pm 5{\cdot}6$
		†$\Delta H_{\text{average}} = 29{\cdot}7 \pm 4$	†$M_{2\text{average}} = 154 \pm 51$
One hydrogen atom within an octahedral vacancy and the other sitting on a first-neighbour tetrahedral site [Fig. 5(*d*)]	r_1	12·5	31·5
	r_2	4·12	3·41
	r_3	2·28	1·04
	r	0·71	0·403
		†$\Delta H_{\text{average}} = 4{\cdot}15$	†$M_{2\text{average}} = 5{\cdot}64$

* The exact geometrical configuration of each pair is shown in Fig. 5, with the value of the interatomic distance r between both hydrogen atoms forming the pair.

† The average values are computed by weighting over all the configurations of one type of pair.

Therefore the characteristics of the system, highlighted by the systematic study of the modification of the lattice constant by hydrogenation and by the n.m.r. experiments are essentially:

(1) The possibility of injecting into the lattice an exceptionally large number of hydrogen atoms (many times the number of vacancies, up to about 8).

(2) The existence of strong correlations between the positions of the hydrogen atoms, for adequate concentrations, these correlations being induced by the vacancies. The detailed understanding of the part played by the concentration of vacancies on these position correlations and on the variation of the lattice parameter would require further experimental investigation. We suggest that a study of the diffusion of the hydrogen atoms with respect to temperature might yield interesting information.

References

ABRAGAM, A. (1961). *The Principles of Nuclear Magnetism.* Oxford: Clarendon Press.

ANDREW, E. R. & BERSOHN, R. (1950). *J. Chem. Phys.* **18**(2), 159.

ARONSON, S. & SADOFSKY, J. (1965). *J. Inorg. Nucl. Chem.* **27**, 1769.

BETSUYAKU, H., TAKAGI, Y. & BETSUYAKU, Y. (1964). *J. Phys. Soc. Japan*, **19**, 1089.

BITTNER, H. (1964). *Mh. Chem.* **95**, 1514.

GORETZKI, H., BITTNER, H. & NOWOTNY, H. (1964). *Mh. Chem.* **95**, 1522.

GORETZKI, H., GANGLBERGER, E., NOWOTNY, H. & BITTNER, H. (1965). *Mh. Chem.* **96**, 1563.

KUBO, R. & TOMITA, K. (1954). *J. Phys. Soc. Japan*, **9**, 888.

ORIANI, R. A., MCCLEMENT, E. & YOUNGBLOOD, J. F. (1957). *J. Chem. Phys.* **27**, 230.

PAKE, G. E. (1948). *J. Chem. Phys.* **16**, 327.

PASCARD, R., LORENZELLI, R. & DEAN, G. (1964). Rapport C.E.A. R 2602.

PETERSON, D. T. & REXER, J. (1962). *J. Inorg. Nucl. Chem.* **24**, 519.

REXER, J. & PETERSON, D. T. (1964). *Proc. AIME, Symposium on 'Compounds of Interest in Nuclear Reactor Technology'*, Boulder, Colorado, Aug. 3–5 1964, *Nucl. Metallurg.* **10**, 327.

RUNDLE, R. E., SHULL, C. G. & WOLLAN, E. O. (1952). *Acta Cryst.* **5**, 22.

SATOW, T. (1967). *J. Nucl. Mat.* **21**, 255.

STALINSKI, B., COOGAN, C. K. & GUTOWSKY, H. S. (1961). *J. Chem. Phys.* **34**(4), 1191.

STALINSKI, B. & ZOGAL, O. J. (1965). *Proc. Colloque International sur les Dérivés Semimétalliques.* Orsay, 1965, p. 483.

TORREY, H. C. (1958). *Suppl. Nuovo Cim.* **9**(1), 95.

YVON, K., NOWOTNY, H. & KIEFFER, (1967). *Mh. Chem.* **98**, 6.

ZACHARIASEN, W. H. (1953). *Acta Cryst.* **6**, 393.

ZAMIR, D. & COTTS, R. M. (1964). *Phys. Rev.* **134**, A666.

ZOGAL, O. J. & STALINSKI, B. (1966). *Proc.* XIV *Colloque Ampère*, p. 432.